Sadeq, D. and Iglauer, S. and Lebedev, M. and Smith, C. and Barifcani, A. 2017. Experimental determination of hydrate phase equilibrium for different gas mixtures containing methane, carbon dioxide and nitrogen with motor current measurements. Journal of Natural Gas Science & Engineering. 38: pp. 59-73.

# Experimental Determination of Hydrate Phase Equilibrium for Different Gas Mixtures Containing Methane, Carbon Dioxide and Nitrogen with Motor Current Measurements

Dhifaf Sadeq[a,d,*], Stefan Iglauer[a], Maxim Lebedev[b], Callum Smith[c] and Ahmed Barifcani [c]

a. Curtin University, Department of Petroleum Engineering, 26 Dick Perry Avenue, 6151 Kensington, Australia.

b. Curtin University, Department of Exploration Geophysics, 26 Dick Perry Avenue, 6151 Kensington, Australia.

c. Curtin University, School of Chemical and Petroleum Engineering, 26 Dick Perry Avenue, 6151 Kensington, Australia.

d. University of Baghdad, College of Engineering, Department of Petroleum Engineering, Baghdad, Iraq

*** Correspondence Author**

E-mail address: Dhifaf.sadeq@postgrad.curtin.edu.au; Dhifaf_js@yahoo.com.au

Mobile: +61426847075

**ABSTRACT**

Hydrate dissociation equilibrium conditions for carbon dioxide + methane with water, nitrogen + methane with water and carbon dioxide + nitrogen with water were measured using cryogenic sapphire cell. Measurements were performed in the temperature range of 275.75K to 293.95K and for pressures ranging from 5 MPa to 25 MPa. The resulting data indicate that as the carbon dioxide concentration is increased in the gas mixture, the gas hydrate equilibrium temperature increases. In contrast, by increasing the nitrogen concentration in the gas mixtures containing methane or carbon dioxide decreased the gas hydrate equilibrium temperatures. Furthermore, the cage occupancies for the carbon dioxide + methane system were evaluated using the Van der Waals and Platteeuw thermodynamic theory with the Langmuir adsorption model and Peng-Robinson equation of state. The data demonstrated the increasing promoting effect of carbon dioxide with its concentration.

In addition, the motor current changes during the hydrate formation and dissociation processes were measured by keeping the rotation speed of the magnetic stirrer that was connected to a DC motor constant. The motor current measurements were reported and it showed that the hydrate plug formation and dissociation could be predicted by the changes in the motor current.

**Keywords:** gas hydrates; equilibrium conditions; methane; nitrogen; carbon dioxide; Motor current measurements.

## Introduction

In recent years, the importance of gas hydrates has significantly increased in the energy sector. Large amounts of natural gas hydrate deposits were discovered beneath the permafrost areas and in deep oceanic sediments (Buffett 2000; Kim et al. 2005; Sloan Jr and Koh 2008). These deposits present an enormous fuel resource (Makogon 2010), ~$2.1\times10^{16}$ $m^3$ methane gas reserves were estimated (Kvenvolden 1988), which is more than double the entire combined world reserves of oil, natural gas and coal (Makogon et al. 2007; Moridis 2008; Sloan Jr and Koh 2008). Therefore, the oil and gas industry are now looking into commercially producing gas from these deposits, and preferably combine this production with the sequestration of carbon dioxide (Goel 2006; Eslamimanesh et al. 2012; Wood 2015). In addition, gas hydrates have received growing attention

because of their role in carbon dioxide capture to reduce carbon dioxide emissions (Dashti et al. 2015; Adeyemo et al. 2010), gas storage (Sun et al. 2003; Taheri et al. 2014) and transportation (Taheri et al. 2014), cool-energy storage (Wood 2015; Xie et al. 2010) and water desalination (Eslamimanesh et al. 2012; Park et al. 2011) .Thus such low temperature, high pressure reservoirs are a potential sink for anthropogenic carbon dioxide storage and climate change may be mitigated via this route (Kvamme et al. 2007). Secondly, gas hydrate formation presents the main flow assurance problem in the oil and gas industry (Sloan Jr and Koh 2008; Haghighi et al. 2009; Englezos 1993). Here gas hydrate particles can agglomerate and build up gradually so that a large mass of hydrate is formed, which can block flowlines, valves, chokes and other production equipment (Sloan et al. 2010; Najibi et al. 2009).

Natural gas hydrates (clathrate hydrates) are solid ice-like, non-stoichiometric structures that consist of water and small gas molecules such as methane, carbon dioxide, nitrogen, ethane, propane or butane (Sloan Jr and Koh 2008; Delli and Grozic 2014; Bishnoi and Natarajan 1996). Clathrate hydrates are classified into three categories based on the arrangement of the water molecules in the crystal structure and the size of the gas molecules (Carroll 2014; Sloan Jr and Koh 2008); structure I (sI), structure II (sII), and hexagonal structure (sH) (Carroll 2014; Sloan Jr and Koh 2008; Sloan 2003). Typically, gas hydrates are formed and stable under high pressure conditions at temperatures above the freezing point of water up to 25 °C if a gas hydrate former (i.e. a gas) and sufficient amount of water are available (Sloan Jr and Koh 2008).

In this context several experimental studies have reported hydrate equilibrium data for various gas mixtures, including for methane, nitrogen and carbon dioxide (Unruh and Katz 1949; Adisasmito, Frank, et al. 1991). Later, Ohgaki et al.(Ohgaki et al. 1993); Fan and Guo (Fan and Guo 1999b); Seo et al. (Seo et al. 2000); Kang et al. (Kang et al. 2001), Seo et al. (Seo et al. 2001), Buruusgaard et al. (Bruusgaard et al. 2008) and Sun et al. (Sun et al. 2015) measured hydrate equilibrium data for $CO_2$ and $CH_4$ or $N_2$ while the $N_2$-$CH_4$ hydrate data were reported by Jhaveri and Robinson (Jhaveri and Robinson 1965) , Lee et al. (Lee et al. 2006) and Mei et al. (Mei et al. 1996). A summary of the experimental hydrate equilibrium data reported in the literature for the $CH_4$+$CO_2$, $CH_4$+$N_2$, $CO_2$+$N_2$ gas mixtures in the presence of water are listed in Table 1.

However, most of the existing experimental data are limited to low and medium pressure conditions, while gas hydrates naturally exist in a high pressure environment. Moreover, natural gas production from deep reservoirs requires hydrate prevention at high pressures: thus reliable and accurate hydrate equilibrium measurements are vital to formulate and validate thermodynamic models for predicting the hydrate forming conditions.

We thus measured hydrate equilibria for various gas mixtures (methane + carbon dioxide), (methane + nitrogen) and (nitrogen + carbon dioxide) for a wide range of temperatures and pressures.

**Table 1**

Review on the gas hydrate equilibrium for $CH_4$+$CO_2$, $CH_4$+$N_2$, $CO_2$+$N_2$ and water systems.

| System | Reference | T/K | P/MPa |
|---|---|---|---|
| $CH_4$+$CO_2$ | (Unruh and Katz 1949) | 275.5 – 285.7 | 1.99 – 7.00 |
| | (Adisasmito, Frank, et al. 1991) | 273.7 – 287.4 | 1.45 – 10.95 |
| | (Dholabhai and Bishnoi 1994) | 277.56-284.84 | 3.41 – 17.90 |
| | (Ohgaki et al. 1993) | 280.3 | 3.04 – 5.46 |
| | (Fan and Guo 1999a) | 273.5 – 282.3 | 1.10 – 4.80 |
| | (Servio et al. 1999) | 273.5-283.1 | 1.7-5.070 |
| | (Seo et al. 2001) | 274.36 – 283.56 | 1.5 – 5.0 |
| | (Beltrán and Servio 2008) | 275.14 –285.34 | 1.92 –7.47 |
| | (Belandria et al. 2010) | 279.1–289.9 | 2.96 –13.06 |
| | (Belandria et al. 2011) | 277.9 –285.5 | 2.72–8.27 |
| | (Herri et al. 2011) | 277.15 | 2.04 – 3.90 |
| | (Sabil et al. 2014) | 272.15 –290.15 | 1.10 –15.29 |
| $CH_4$+$N_2$ | (Jhaveri and Robinson 1965) | 282.8 – 294.4 | 7.40 – 35.96 |
| | (Mei et al. 1996) | 273.2 – 279.8 | 2.64 – 32.42 |
| | (Lee et al. 2006) | 273.30 –285.05 | 8.325 –20.70 |
| $CO_2$+$N_2$ | (Fan and Guo 1999a) | 273.1 – 280.2 | 1.22 – 3.09 |
| | (Kang et al. 2001) | 273.75 – 284.25 | 1.565 – 32.308 |
| | (Linga et al. 2007) | 273.7 | 1.6 –7.7 |
| | (Bruusgaard et al. 2008) | 275.00 – 283.00 | 2.0 – 22.4 |
| | (Kim et al. 2011) | 276.88 –285.41 | 5.0 –20.0 |
| | (Herri et al. 2011) | 273.40 –281.10 | 5.60 – 6.10 |
| | (Sfaxi et al. 2012) | 278.1–285.3 | 3.24 –29.92 |
| | (Sun et al. 2015) | 273.4 – 278.4 | 5.28 – 17.53 |

## 2. Experimental Methodology

### *2.1. Materials and gas preparation*

Methane (purity 99.995 mol%), carbon dioxide (purity 99.9 mol%) and nitrogen (purity (99.99 mol%), all supplied by BOC Australia, were used as received or gas mixtures were prepared by mass balance as follows: empty 500 mL stainless steel bottles (Whitey DOT-3E1800 12EK082) were vacuumed using an Edwards Rotation pump (Model E2M2) for 30 min and then weighed using a high-precision electronic balance (Shimadzu model UW6200H, accuracy = 0.01 g). The vacuumed bottles were then filled with the gas(es) from the main cylinders and reweighed. The weight of the empty bottle was 1350 g. The weight difference was then converted into mole percentage, Table 2. Two gas sensors (PolyGard manufactured by MSR) measured $CO_2$ and $CH_4$ concentrations in the gas mixtures with standard uncertainty of ±0.05. Deionized water (electrical resistivity of 18 MΩ.cm at 25 $^oC$) was used as the aqueous phase.

**TABLE 2**

Gas mixtures used in this study.

| Component | Mixture No. | | | | | | | | | |
|---|---|---|---|---|---|---|---|---|---|---|
| Mol% | 1 | 2 | 3 | 4 | 5 | 6 | 7 | 8 | 9 | 10 |
| $CH_4$% | 100 | 90 | 84 | 80 | 90 | 80 | 69 | 64 | | |
| $CO_2$% | | 10 | 16 | 20 | | | | | 26 | 36 |
| $N_2$% | | | | | 10 | 20 | 31 | 36 | 74 | 64 |

### *2.2. Experimental apparatus and procedure*

A high pressure apparatus (Sanchez Technology, France) comprising of a sapphire cell (60 ml inner volume), piston pump and pneumatic booster pump (Haskel, model AA-30), valves and connection tubing was employed for the experiments (Figure 1). The temperature of the cell was carefully controlled with a

chiller (R2G2, Model R130A3-P4) and electric heater, respectively. Furthermore two thermometer (RTD PT100 sensor with 3 core Teflon tails, Model TC02 SD145) were positioned in contact with liquid and gas at the top and bottom of the sapphire cell and thus measured liquid and gas temperatures. The pressure inside the sapphire cell was measured with a pressure sensor (Sanchez). The Maximum uncertainty of pressure and temperature measurements were ±0.05 MPa and 0.1 K, respectively. All cell contents were continuously mixed with an electric stirrer (550 rpm) driven by a DC motor (equipped with variable speed drive). Note that through magnetic coupling the load on the motor was reduced when solid hydrate formed in the cell. The electrical current required to maintain a constant motor speed was measured, and it is proportional to the torque load on the impeller.

Hydrate formation and dissociation processes in the sapphire cell were observed visually using two Sony Digital cameras (Model SSS-DC 18P, 1/3 inch colour DSP CCD with 470TV lines of horizontal resolution) located outside the cell. Cooling and heating cycles were started by operating the refrigeration compressor or electrical heater respectively. During each experiment, pressure, temperature and motor current were continuously recorded at a rate of 12 point per minute.

In all experiments, the gas steel bottles were fitted into the gas manifold in order to transfer the gas through the piston pump to the PVT sapphire cell. Then, approximately 5 ml of deionized water was initially charged into the evacuated clean sapphire cell. Subsequently, the gas mixture was introduced into the sapphire cell from the fitted steel bottles via the piston pump. The cell was then pressurized by a pneumatic pump (Haskel, model AA-30) in combination with a piston pump (Sanchez). Once the prescribed pressure was reached, the stirrer was switched on and cooling was started at a rate of approximately 2 K/hr until hydrate (formation) was visually observed. The cooling process was stopped when complete hydrate crystallization was achieved. The cell was then heated at a rate of 2 K/hr in order to start the hydrate dissociation process. The gas hydrate dissociation temperatures, pressures and stirrer currents were measured during the experiments. All experiments were repeated for each gas mixture at 5, 7.5, 10, 15, 20 and 25 MPa and for the temperature range of 275.75K to 293.95K. Moreover, the repeatability of the hydrate experimental data were determined by performing the experiment three times for the methane hydrate and two times for some randomly selected experiments, closely matching results were obtained. The statistical analysis of the obtained experimental data show a maximum experimental error of 1.65%.

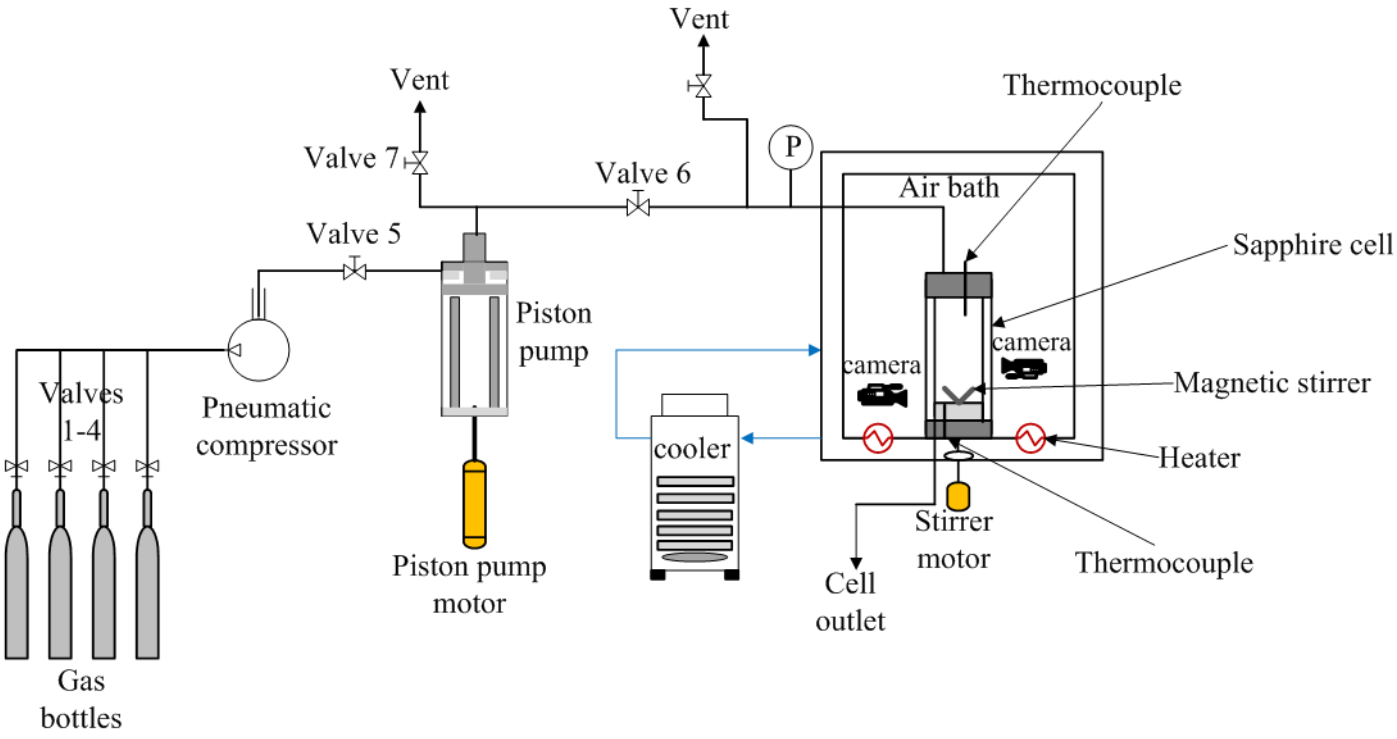


**Fig. 1**. Schematic of the PVT Sapphire Cell

The PVT sapphire cell apparatus was used to measure the hydrate dissociation conditions by employing the temperature search method as an experimental determination technique (Kim et al. 2011; Loh et al. 2012; Smith et al. 2015; AlHarooni et al. 2015; Smith et al. 2016). Experimentally, the PVT cell was maintained at a constant pressure using the piston pump and keeping the valve to the PVT cell open. Because of that the hydrate formation conditions depend on various factors (induction time, rate of cooling and memory effect), have a high degree of variance compared to the dissociation conditions and represent a fixed thermodynamic property, thus the dissociation is considered as the hydrate equilibrium conditions (Tohidi et al. 2000). Hydrate dissociation conditions for the carbon dioxide + methane, nitrogen + methane and carbon dioxide + nitrogen gas mixtures were measured for the temperature and pressure ranges of 275.75K to 293.95K and 5 MPa to 25 MPa, respectively. In addition, the motor current measurement were used as an indication of gas hydrate plug formation and dissociation.

## 3. Cage occupancies

The occupancies of the sI hydrate cavities are evaluated based on the fact that at equilibrium the chemical potential of water in the hydrate phase ($\mu_w^H$) equates to the chemical potential of water in the liquid phase ($\mu_w^L$).

$$\mu_w^H = \mu_w^L \qquad (1)$$

Therefore, the chemical potential difference of water in the hydrate phase is equal to the chemical potential difference of water in the liquid phase. Water molecules adopt the formation of a lattice due to a lowering of Gibbs free energy, hence the change in chemical potential from a hypothetical empty hydrate lattice (superscript $\beta$) to an occupied lattice (i.e. hydrate, superscript ($H$) can be expressed as:

$$\Delta\mu_w^H = \Delta\mu_w^L = \mu_w^H - \mu_w^\beta = \mu_w^\beta - \mu_w^L \qquad (2)$$

The fractional occupancy of each hydrate cavity type is calculated based on the Langmuir adsorption approach. The occupancy of hydrate former '$i$' in cavity type '$j$' is a function of the fugacity of '$i$', $f_i$ (evaluated with the Peng – Robinson equation of state), and the Langmuir Constant for a specified $i - j$ combination, $C_{i,j}$.

$$\theta_{i,j} = \frac{C_{i,j}f_i}{1+\sum_i C_{i,j}f_i} \qquad (3)$$

Using the Lennard – Jones – Devonshire cell potential theory, a relationship describing $C_{i,j}$ in terms of the cell potential, ω(r), was put forward by Van der Waals and Platteeuw (Van der Waals and Platteeuw 1959).

$$C_{i,j} = \frac{4\pi}{kT}\int_0^R \exp\left(\frac{\omega(r)}{kT}\right) r^2 dr \qquad (4)$$

The Lennard – Jones – Devonshire theory takes the average of the potentials between solute (i.e. hydrate former) and water. It takes into account the coordination of the solute to water molecules for a particular cavity type, $z_j$, which is 20 for the small $5^{12}$ cavity and 24 for the large $5^{12}6^2$ cavity (Sloan Jr and Koh 2008). Parameters $k$ and $T$ represent the Boltzmann constant and temperature respectively. The cell potential is given according to the following equations:

$$\omega(r) = 2z_j e\left[\frac{\sigma^{12}}{R_j^{11}r}\left(\delta^{10} + \frac{a}{R_j}\delta^{11}\right) - \frac{\sigma^6}{R_j^5 r}\left(\delta^4 + \frac{a}{R_j}\delta^5\right)\right] \qquad (5)$$

$$\delta^N = \frac{1}{N}\left[\left(1 - \frac{r}{R_j} - \frac{a}{R_j}\right)^{-N} - \left(1 + \frac{r}{R_j} - \frac{a}{R_j}\right)^{-N}\right] \qquad (6)$$

Cell potential is a function of the distance, r, between the guest molecule and the centre of the cavity. The constants $a$, $e$ and $\sigma$ are experimentally fitted parameters, or Kihara parameters, that are unique for every hydrate former and $R_j$ is the radius of the cavity '$j$'. Values of 3.95 and 4.33 Å are used for the small and large cavities respectively (Lederhos et al. 1993). The remaining parameter values used for this study are given in Table 3 (Erickson 1983).

The change in the chemical potential of water from an unoccupied water lattice to a hydrate structure can be used with the previous formulations to calculate occupancies at the experimentally determined equilibrium conditions. This chemical potential change is given by,

$$\Delta\mu_w^H = \mu_w^H - \mu_w^\beta = RT\sum_j v_j \ln\left(1 - \sum_i \theta_{i,j}\right) \qquad (7)$$

Where $v_j$ is the number of '$j$' cavities per water molecule ($v_j$ = 1/23 and $v_j$ = 3/23 for small cavities and large cavities respectively) (Sloan Jr and Koh 2008). Experimentally determined estimates of $\Delta\mu_w^H$ have previously been suggested. A value of -1264 J/mol provided by Erickson (Erickson 1983) was applied in this study, permitting the evaluation of methane and carbon dioxide occupancies.

**TABLE 3**

Kihara Potential Parameters

| Guest | a, Å | σ, Å | e/k, K |
|---|---|---|---|
| $CH_4$ | 0.3834 | 3.14393 | 155.593 |
| $CO_2$ | 0.6805 | 2.97638 | 175.405 |

## 4. Results and discussion

### *4.1 Gas hydrate equilibrium conditions*

Initially the accuracy of the experimental results was checked by measuring the equilibrium conditions for pure methane and the gas mixture containing 20 mol% $CO_2$ and 80 mol% $CH_4$, figures 2 and 3; and our data are in good agreement with the literature data (Adisasmito, Frank, et al. 1991; Beltrán and Servio 2008; Dholabhai and Bishnoi 1994; Lu and Sultan 2008; Mohammadi et al. 2005; Sabil et al. 2014; Servio et al. 1999; Nakamura et al. 2003; Jhaveri and Robinson 1965; Seo et al. 2001).

The measured hydrate data are listed in Tables 4-6 and plotted in figures 4-6. Figure 4 shows the equilibrium conditions for the $CO_2$-$CH_4$ gas mixture. As expected the $CO_2$-$CH_4$ hydrate equilibrium curves are located between the equilibrium curves of pure $CO_2$ (Sloan Jr and Koh 2008; Ohgaki et al. 1993) and pure methane. Furthermore, as the $CO_2$ concentration increased in the $CO_2$-$CH_4$ mixture, the equilibrium temperature also increased, approaching the curve for pure $CO_2$. It can also be seen from figure 4 that the measured CO2-CH4 hydrate data in this work show similar trend with the data available in the literature (Ohgaki et al. 1993; Adisasmito, Frank, et al. 1991; Fan and Guo 1999b).

An analogue scenario was observed for the $N_2$-$CH_4$ system, Figure 5. Again the equilibrium curves of the $N_2$-$CH_4$ mixture are located in between the curves for pure $N_2$ (Van Cleeff and Diepen 1960) and pure

$CH_4$, and the gas hydrate equilibrium temperature decreased with increasing $N_2$ concentration, approaching the $N_2$ curve. Jhaveri and Robinson (Jhaveri and Robinson 1965), Mei etal. (Mei et al. 1996) and Lee et al. (Lee et al. 2006) observed a similar behaviour. This is due to the dilution effect of nitrogen, which leads to a lower hydrate temperature.

This behaviour was again observed for the carbon dioxide - nitrogen mixtures, Figure 6; the presence of $CO_2$ in the $CO_2$-$N_2$ mixture led to increasing hydrate equilibrium temperature. The equilibrium curve of 64 mol% nitrogen (36 mol % carbon dioxide) is closer to the pure carbon dioxide curve than the pure nitrogen curve. This phenomenon was also observed by Seo et al. (Seo et al. 2000), who explained that this behaviour is due to the competition of $CO_2$ and $N_2$ molecules for optimum occupancy of the hydrate structure. Mechanistically, during the hydrate formation process, $CO_2$ molecules occupy small and large cavities in the hydrate structure. While $N_2$ molecules fill the other unoccupied cavities. Figure 6 also shows that the $N_2$-$CH_4$ data reported in this work are in comparable to the behaviour of those in the literature (Kang et al. 2001). Figures 7-9 show plots of ln P vs. 1/T for the experimental data obtained in this work, which show a good linear relationship.

**TABLE 4**

The measured hydrate dissociation data of $CO_2$+$CH_4$ gas mixture in water.

| P/MPa | T/K $CO_2$ mol%= 0 | T/K $CO_2$ mol%=10 | T/K $CO_2$ mol%=16 | T/K $CO_2$ mol%=20 |
|---|---|---|---|---|
| 5 | 279.45 | 280.55 | 281.45 | 282.05 |
| 7.5 | 283.25 | 283.95 | 284.95 | 285.55 |
| 10 | 285.75 | 286.75 | 287.35 | 287.95 |
| 15 | 289.05 | 289.65 | 290.55 | 290.85 |
| 20 | 291.18 | 291.8 | 292.25 | 292.75 |
| 25 | 292.95 | 293.35 | 293.5 | 293.95 |

**TABLE 5**

The measured hydrate dissociation data of $N_2$+$CH_4$ gas mixture in water.

| P/ MPa | T/K $N_2$ mol%= 0 | T/K $N_2$ mol%=10 | T/K $N_2$ mol%=20 | T/K $N_2$ mol%=31 | T/K $N_2$ mol%=36 |
|---|---|---|---|---|---|
| 5 | 279.45 | 278.65 | - | 277.8 | 276.75 |
| 7.5 | 283.25 | 282.8 | 282.15 | 281.6 | 280.35 |
| 10 | 285.75 | 285.15 | 284.85 | 284.25 | 282.95 |
| 15 | 289.05 | 288.85 | 288.25 | 287.85 | 286.3 |
| 20 | 291.18 | 290.85 | 290.35 | 289.85 | 288.8 |
| 25 | 292.95 | 292.75 | 291.5 | 291.25 | 290.15 |

**TABLE 6**

The measured hydrate dissociation data of $N_2$+$CO_2$ gas mixture in water.

| P/ MPa | T/K $N_2$ mol%= 64 | T/K $N_2$ mol%=74 |
|---|---|---|
| 5 | 277.8 | 275.75 |
| 7.5 | 280.1 | 278.65 |
| 10 | 281.6 | 280.6 |
| 15 | 283.3 | 282.75 |
| 20 | 284.45 | 283.9 |

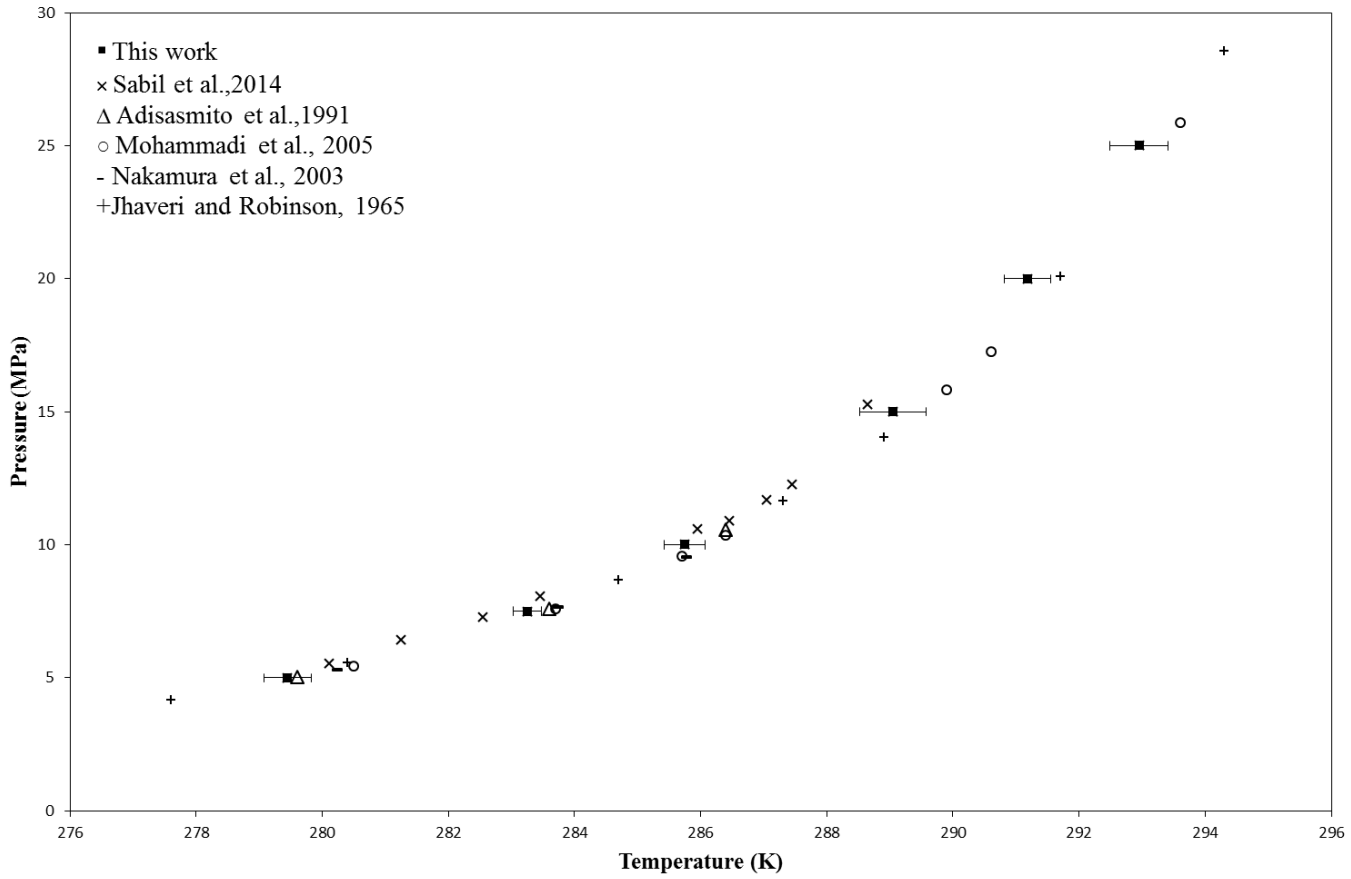


**Fig. 2.** Comparison of $CH_4$ hydrate dissociation points (black square: experimental data; open symbols: literature data (Sabil et al. 2014; Adisasmito, Frank III, et al. 1991; Mohammadi et al. 2005; Nakamura et al. 2003; Jhaveri and Robinson 1965)).

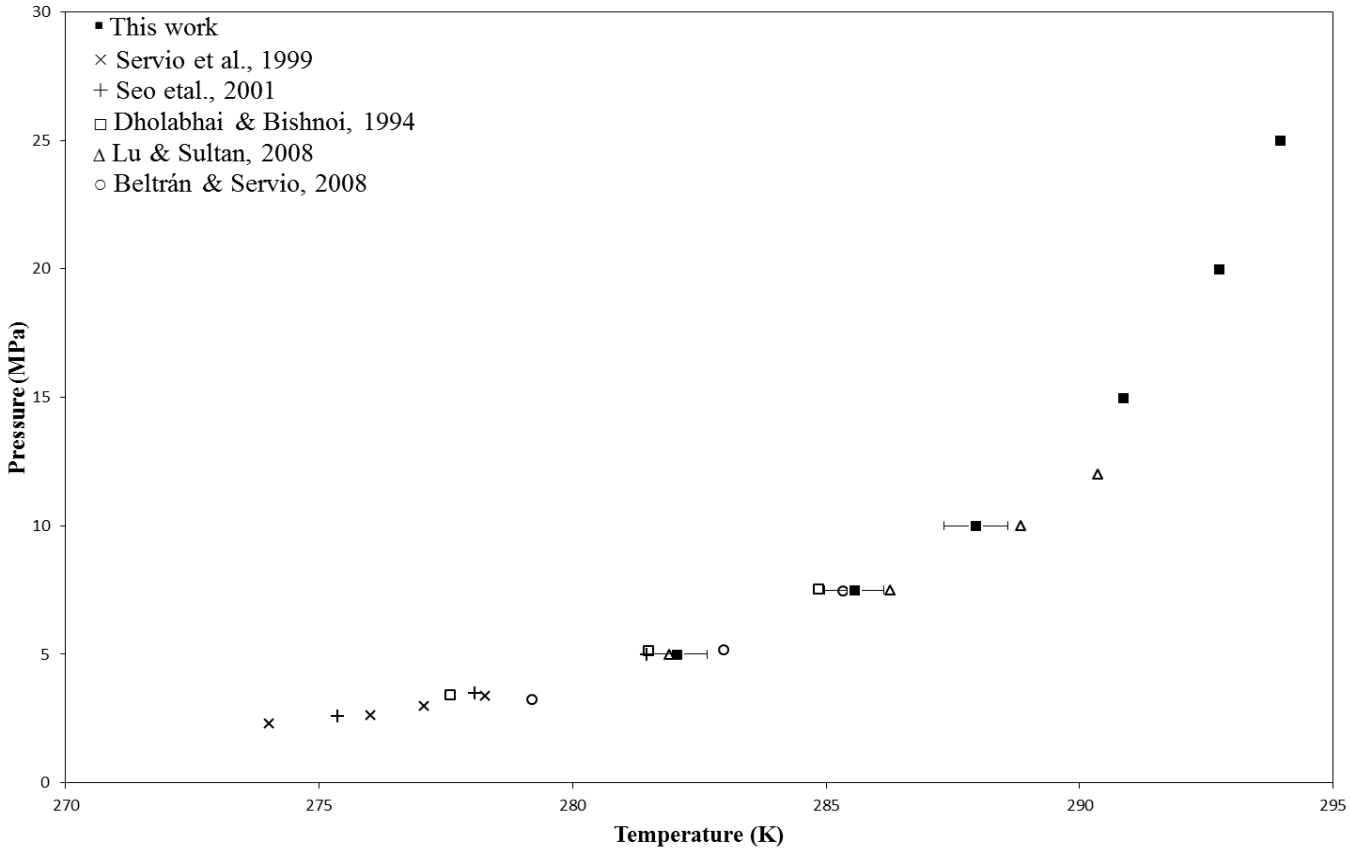


**Fig. 3.** Comparison of 80 mol% methane and 20 mol% carbon dioxide hydrate dissociation points (black square: experimental data; open symbols: literature data (Servio et al. 1999; Seo et al. 2001; Dholabhai and Bishnoi 1994; Lu and Sultan 2008; Beltrán and Servio 2008)).

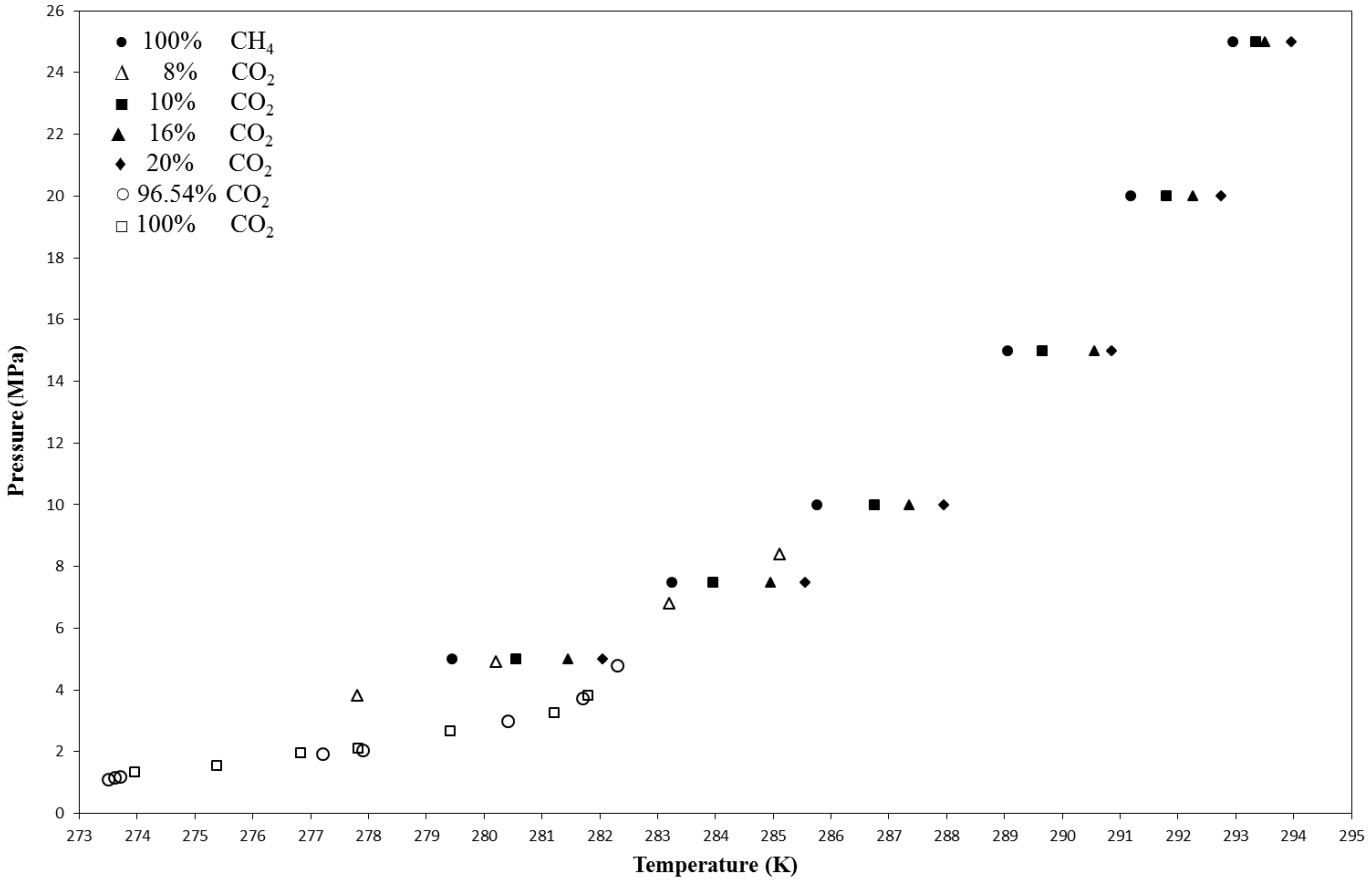


**Fig. 4.** $CO_2$-$CH_4$ hydrate equilibrium curves. Closed Symbols represent our experimental data and open symbols literature data: Pure carbon dioxide reported by Ohgaki et al. (Ohgaki et al. 1993); 8% carbon dioxide reported by Adisasmito et al. (Adisasmito, Frank, et al. 1991); 96.54% carbon dioxide reported by Fan and Guo (Fan and Guo 1999b). Numbers indicate gas mole in the mixture.

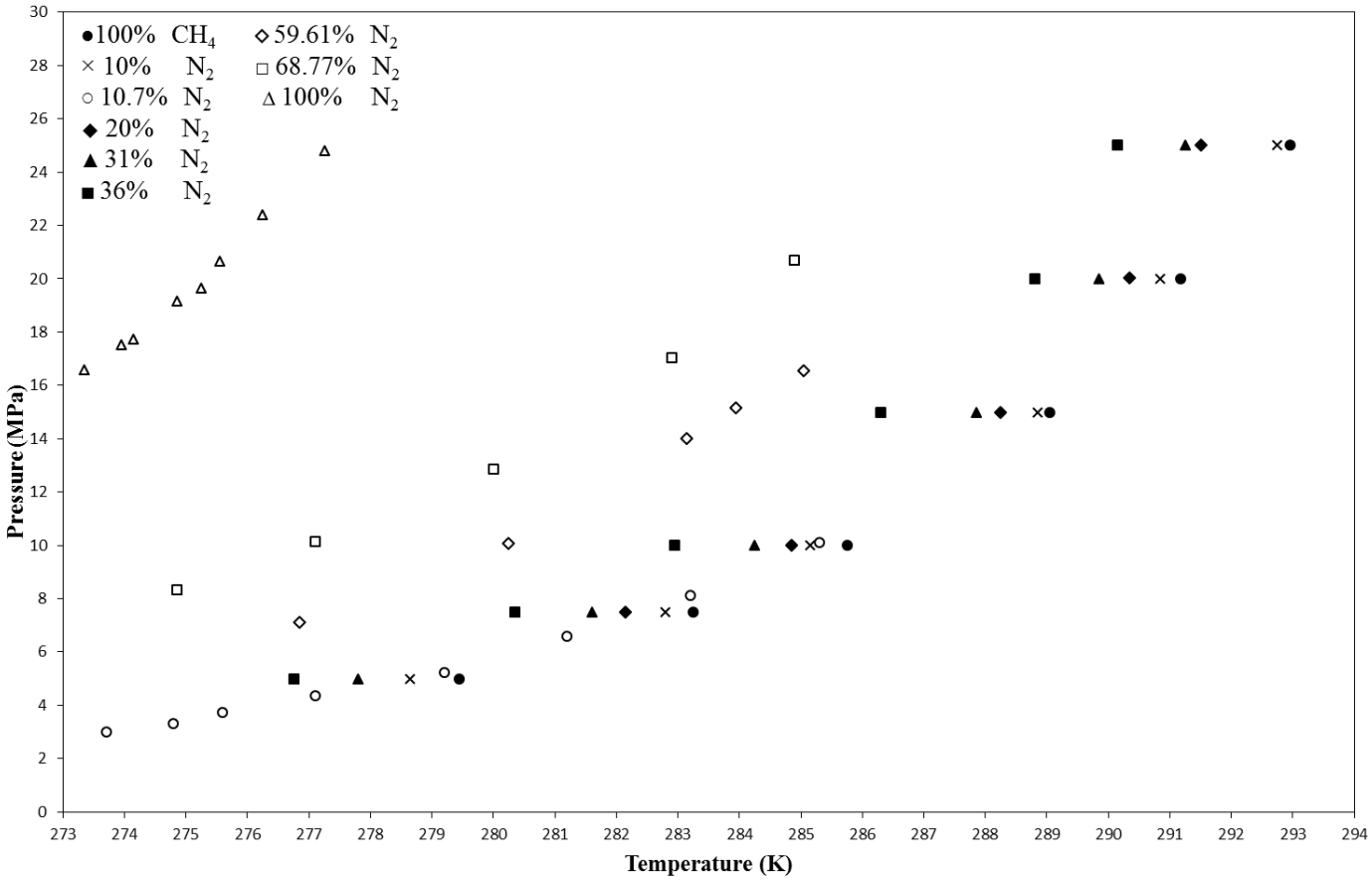


**Fig. 5.** $N_2$-$CH_4$ hydrate equilibrium curves. Closed Symbols represent experimental data and open symbols literature data: pure nitrogen reported by Van Cleeff and Diepen (Van Cleeff and Diepen 1960); 10.7% nitrogen reported by Mei et al. (Mei et al. 1996); 59.61% nitrogen reported by Lee et al (Lee et al. 2006); 68.77% nitrogen reported by Lee et al. (Lee et al. 2006). Numbers indicate gas mole percentage in the mixture.

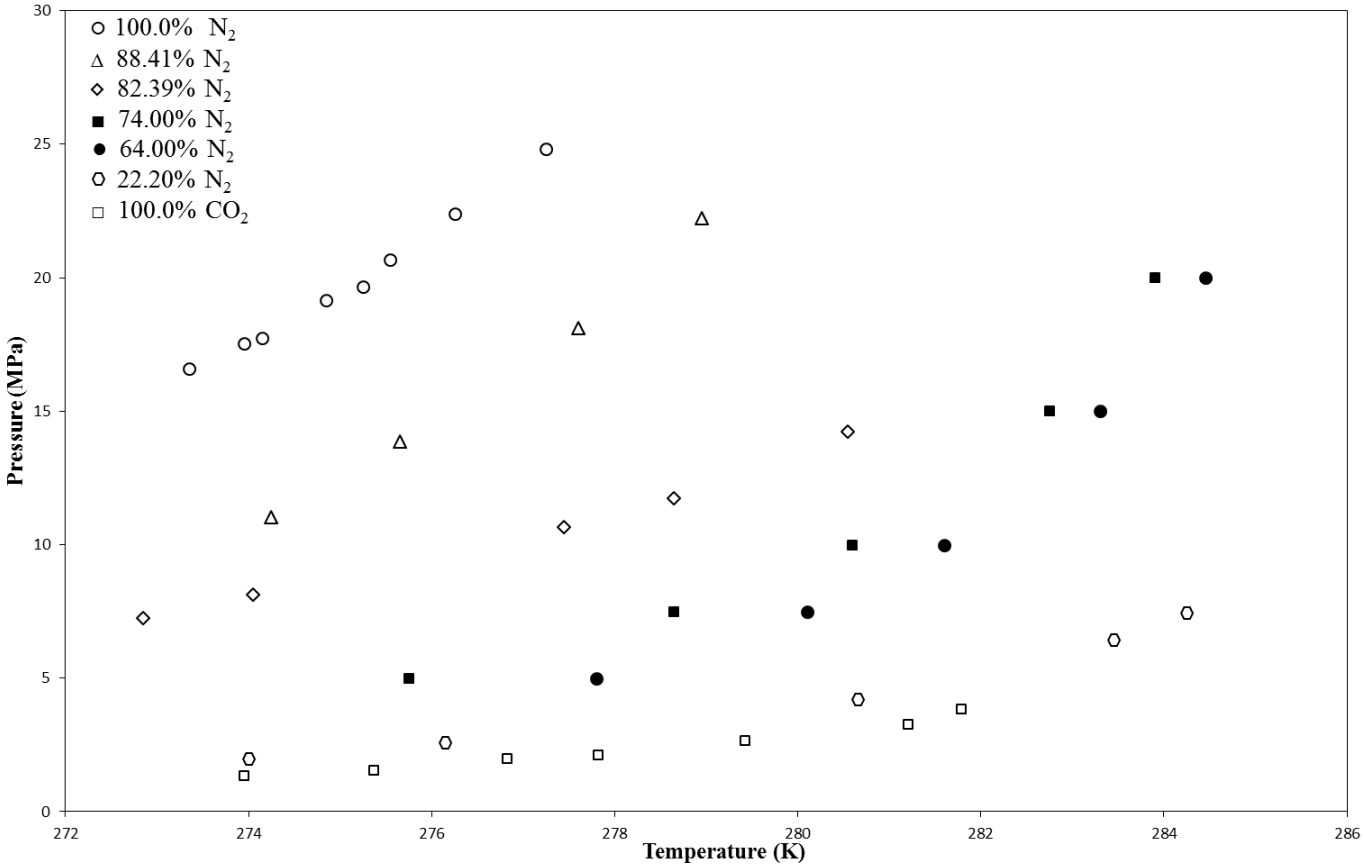


**Fig. 6.** $CO_2$-$N_2$ hydrate equilibrium curves. Closed Symbols represent experimental data and open symbols literature data: pure nitrogen reported by Van Cleeff and Diepen (Van Cleeff and Diepen 1960); pure carbon dioxide reported by Ohgaki et al. (Ohgaki et al. 1993); 88.41% nitrogen reported by Kang et al. nitrogen (Kang et al. 2001); 82.39% nitrogen reported by Kang et al. (Kang et al. 2001); 22.2% nitrogen reported by Kang et al. (Kang et al. 2001). Numbers indicate gas mole percentage in the mixture.

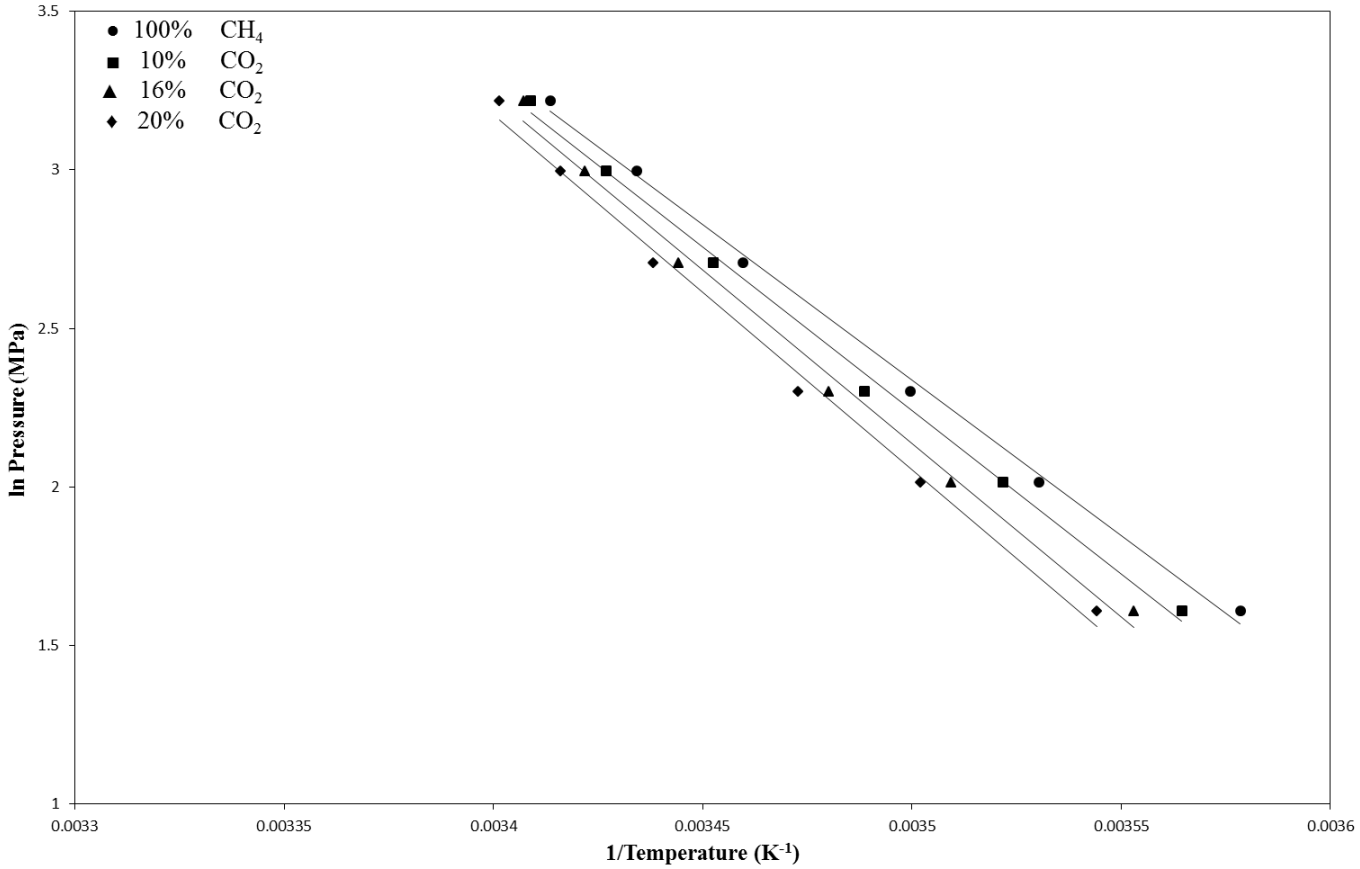


**Fig. 7.** Experimental $CO_2$-$CH_4$ hydrate equilibrium data in ln Pressure versus 1/Temperature plot. Numbers indicate gas mole percentage in the mixture used in this study.

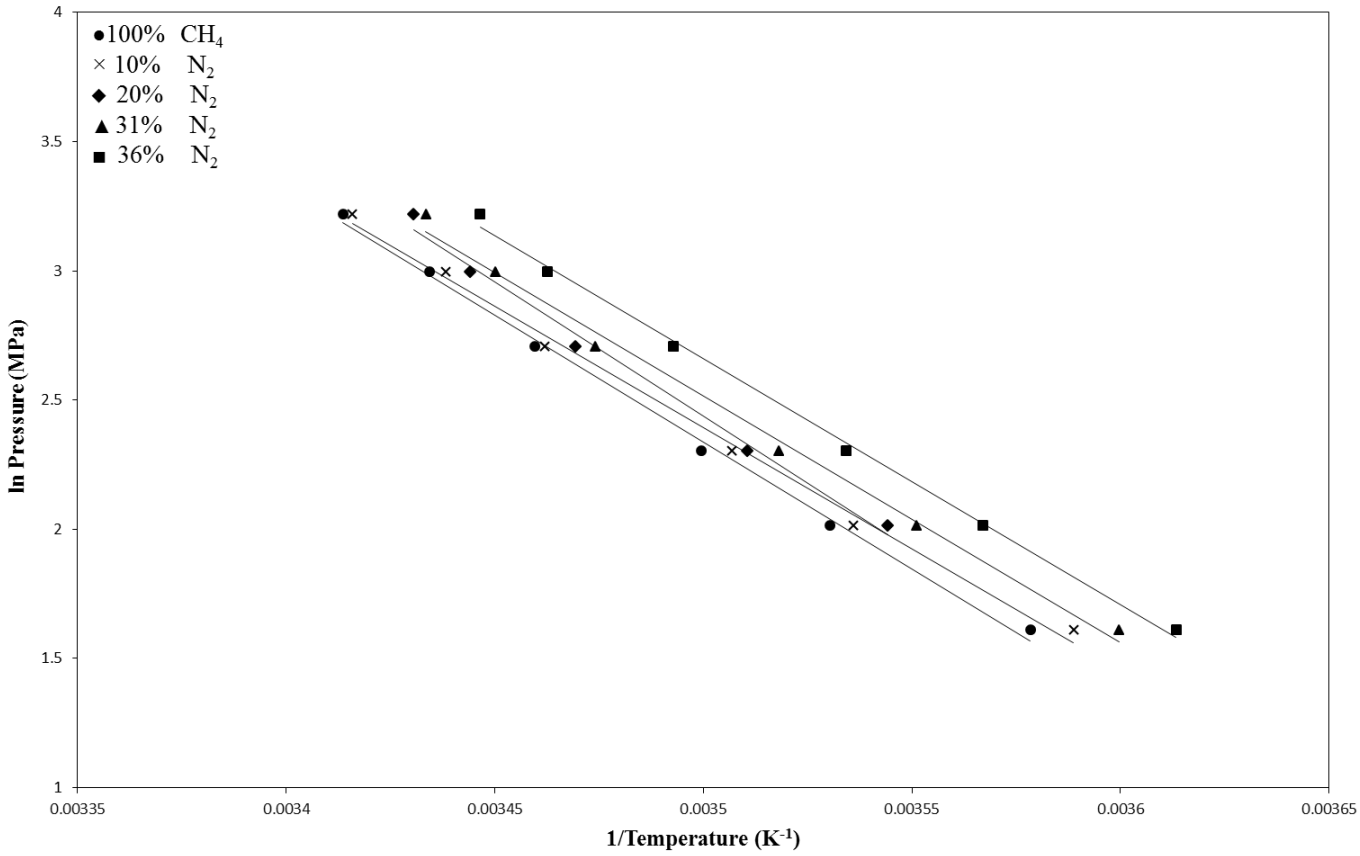


**Fig. 8.** Experimental $N_2$-$CH_4$ hydrate equilibrium data in ln Pressure versus 1/Temperature. Numbers indicate gas mole percentage in the mixture used in this study.

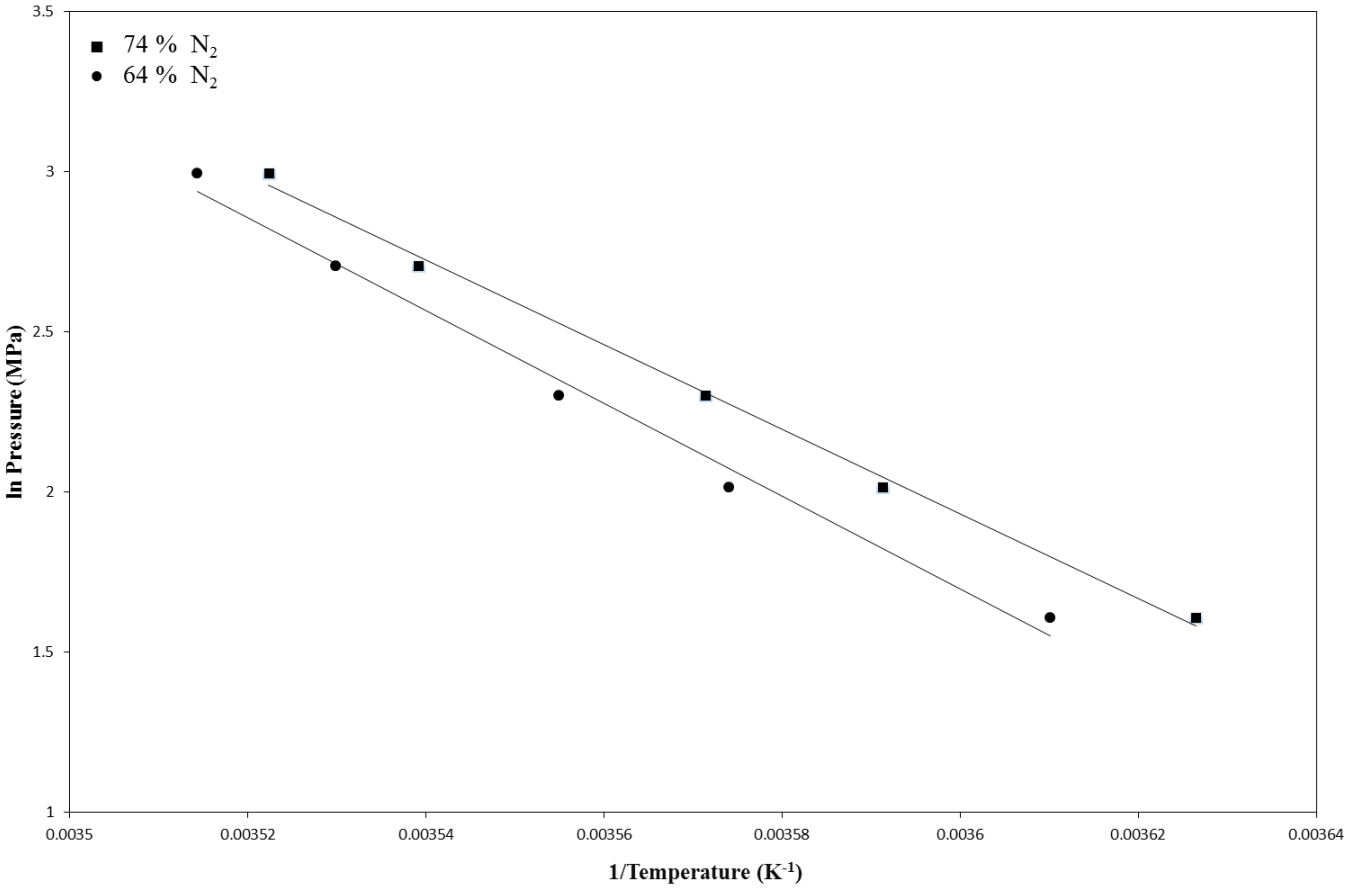


**Fig. 9.** Experimental $CO_2$-$N_2$ hydrate equilibrium data in ln Pressure versus 1/Temperature. Numbers indicate gas mole percentage in the mixture used in this study.

*3.2 Current as an indication of hydrate plug and dissociation*

In this work, visual observation was employed to measure the hydrate dissociation condition. In some experiments this technique is not available, especially in the case of that the experimental cell is not visual. Therefore, the motor current changes during the hydrate formation/ dissociation process can be related to the hydrate plug formation and dissociation. The motor current is a function of the torque required to mix the sapphire cell contents; once a hydrate plug is formed, the torque and thus the motor current increases due to the increasing the load on the stirrer.

The stirrer motor current as a function of experimental time was measured in a set of experiments as shown in figures 10-13. Clearly, the motor current changes during hydrate formation and dissociation. Initially, the motor current remains constant, but then increases dramatically until it reaches a maximum. This maximum indicates the presence of the full plug of the gas hydrate. However, once the solid plug hydrate was formed, the motor current decreased rapidly due to slippage of the stirrer on the magnetic coupling. After dissociation began, the stirrer started rotating again due to the magnetic stirrer was reconnected to the motor and a small spike in the motor current was observed. Therefore, there is no significant current change before

hydrate plug formation, while current changed significantly once the full hydrate plug was formed. The hydrate behaviour as indicated by the motor current was consistent with independent visual observations. We conclude that the motor current can be used as a hydrate formation and dissociation criterion.

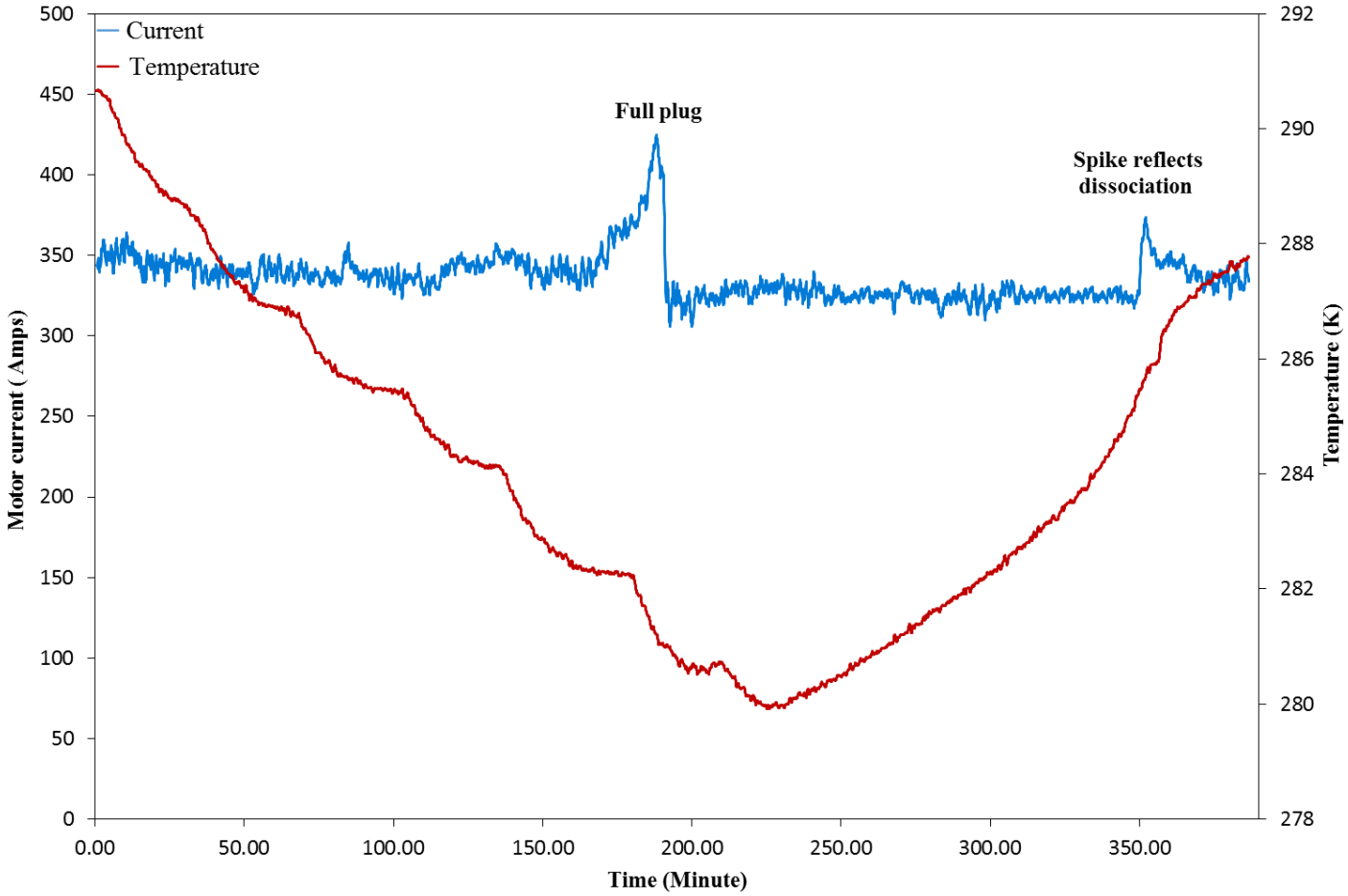


**Fig. 10.** Motor current and temperature vs time during hydrate formation/dissociation process for pure $CH_4$, the pressure was 10 MPa.

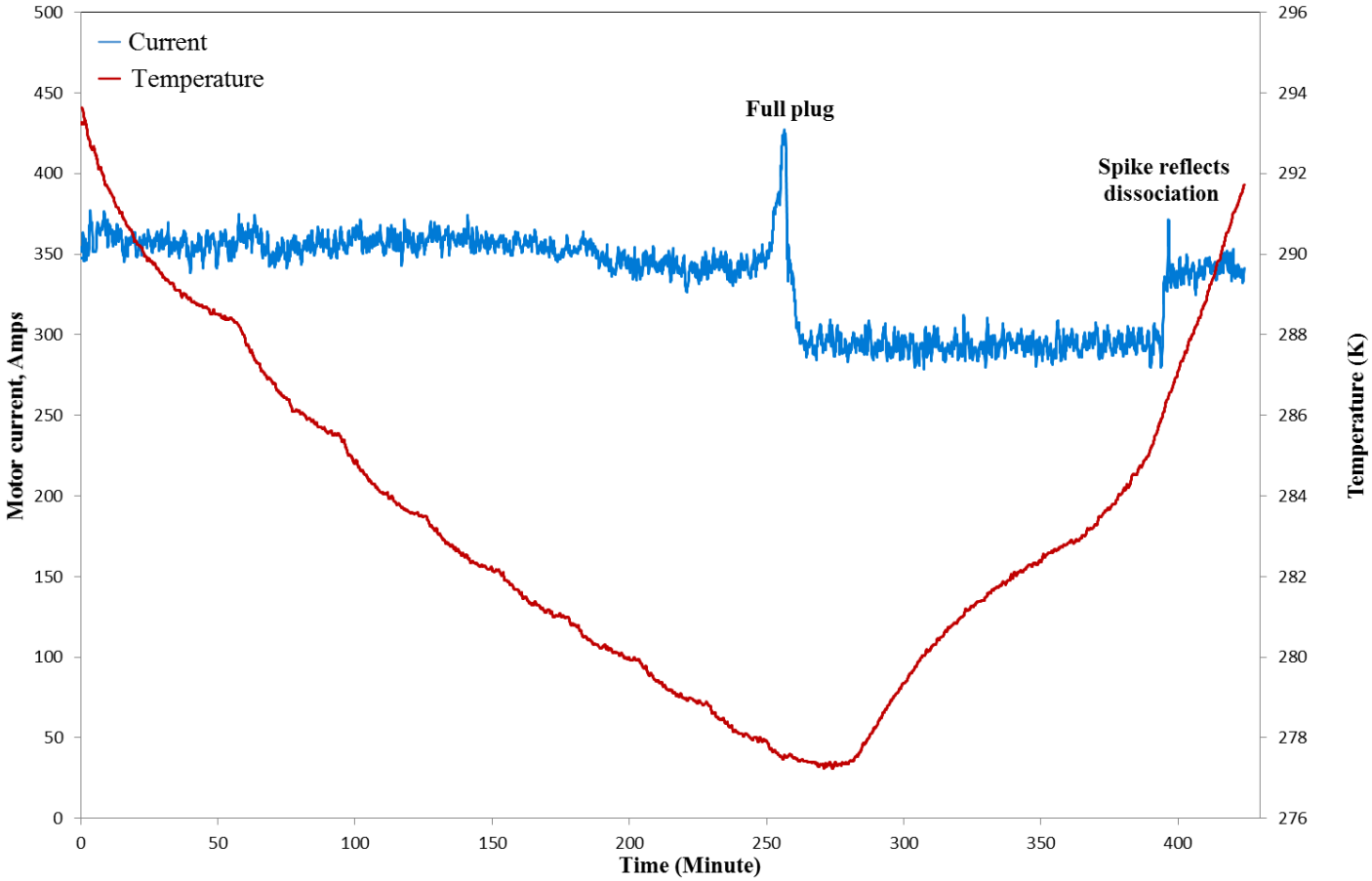


**Fig. 11.** Motor current and temperature vs time during hydrate formation/dissociation process for a 10% $CO_2$+90% $CH_4$ gas mixture at a pressure of 10 MPa.

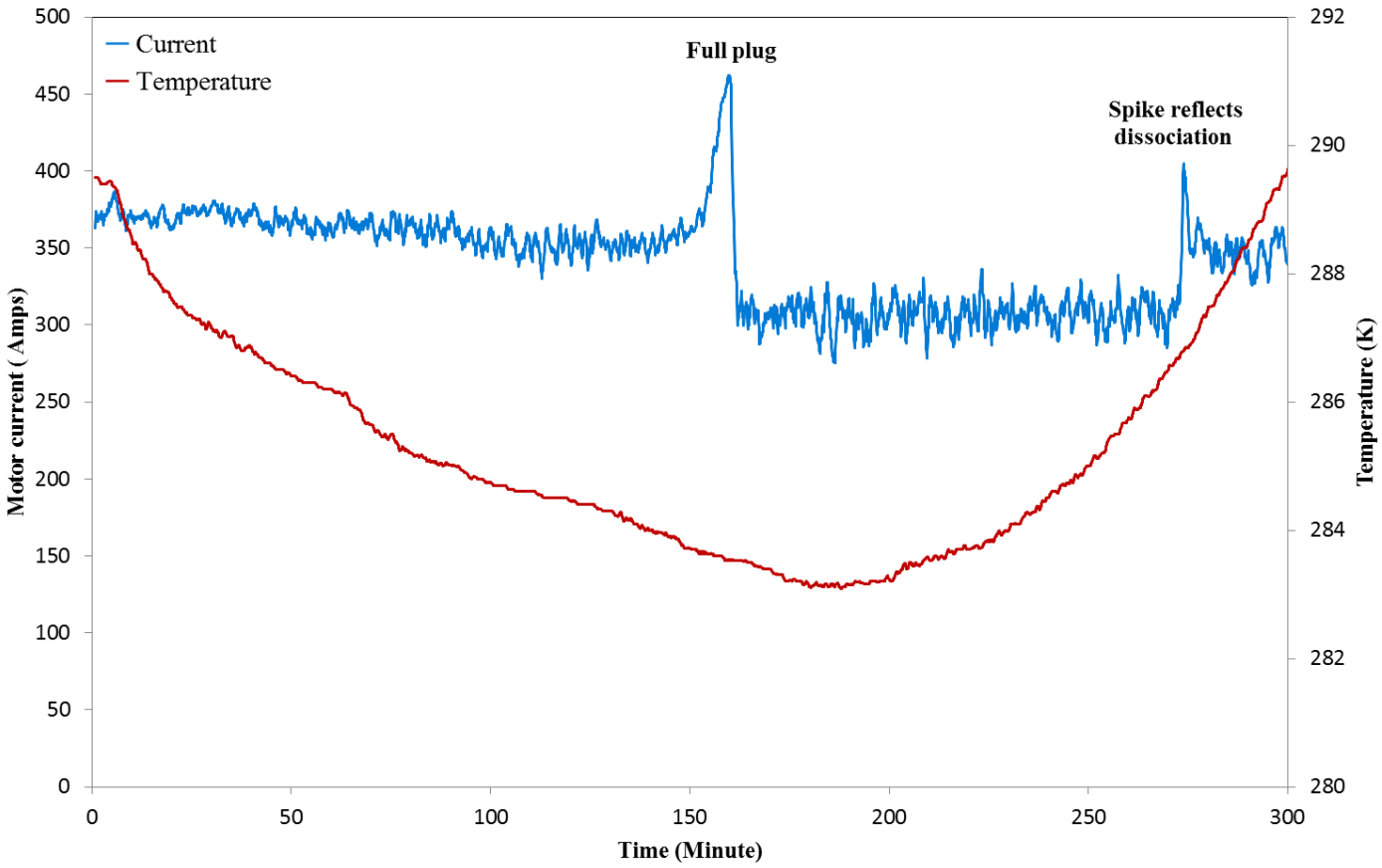


**Fig. 12.** Motor current and temperature vs time during hydrate formation/dissociation process for a 16% CO2+84% CH4 gas mixture at a pressure of 10 MPa.

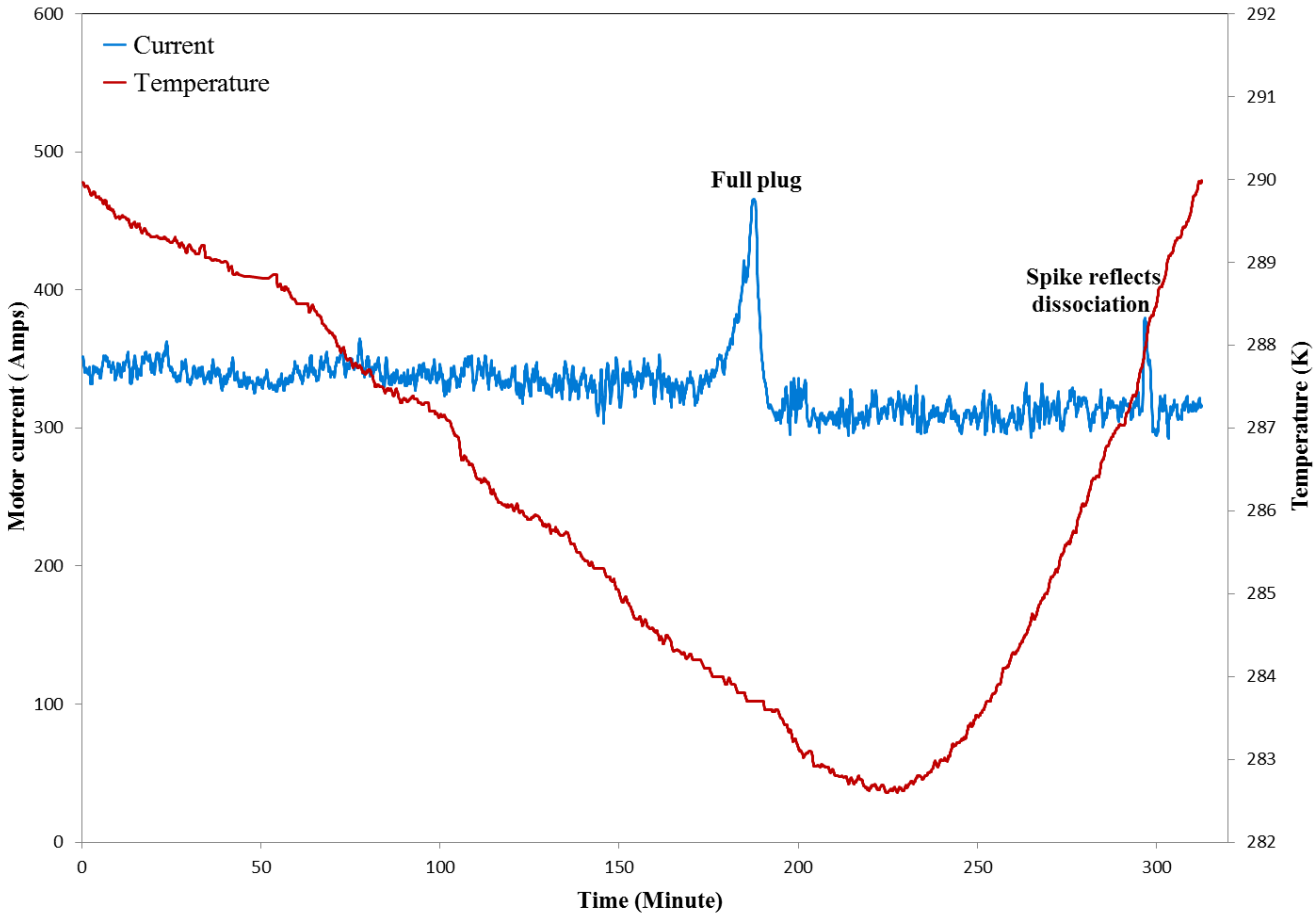


**Fig. 13.** Motor current and temperature vs time during hydrate formation/dissociation process for an 80 % $CH_4$ + 20 % $CO_2$ gas mixture at a pressure of 10 MPa.

Figure 11 shows a series of images which were captured during the hydrate formation process in the PVT sapphire cell. During cooling and when the temperature reached 2-4 degree below the hydrate dissociation temperature, hydrate formation started at the liquid-gas interface (Figure 11a), consistent with Tohidi et al. (Tohidi et al. 2001) and Ueno et al. (Ueno et al. 2015).

With continuing progress in the experiment, hydrate particles grew gradually on the surface area and then built up towards the centre (Figure 14b). Later, the hydrate particles increased in size and migrated into the liquid phase, which shrank due to hydrate growth (Figure14c-e). However, the PVT cell content was still flowing and no apparent change in the motor current was observed during this period. Gas hydrates continued to grow until all liquid was consumed. At this stage, the motor current began to increase dramatically until it reached the maximum value. Once the solid hydrate plug formed (Figure14 f), the magnetic stirrer stopped moving, and the hydrate completely blocked the system causing a rapid decrease in the current. During the

heating process, the gas hydrate started dissociating and gas bubbles appeared in the solid phase (Figure 14g). At this point the stirrer started to move again and a small increase in the current was measured.

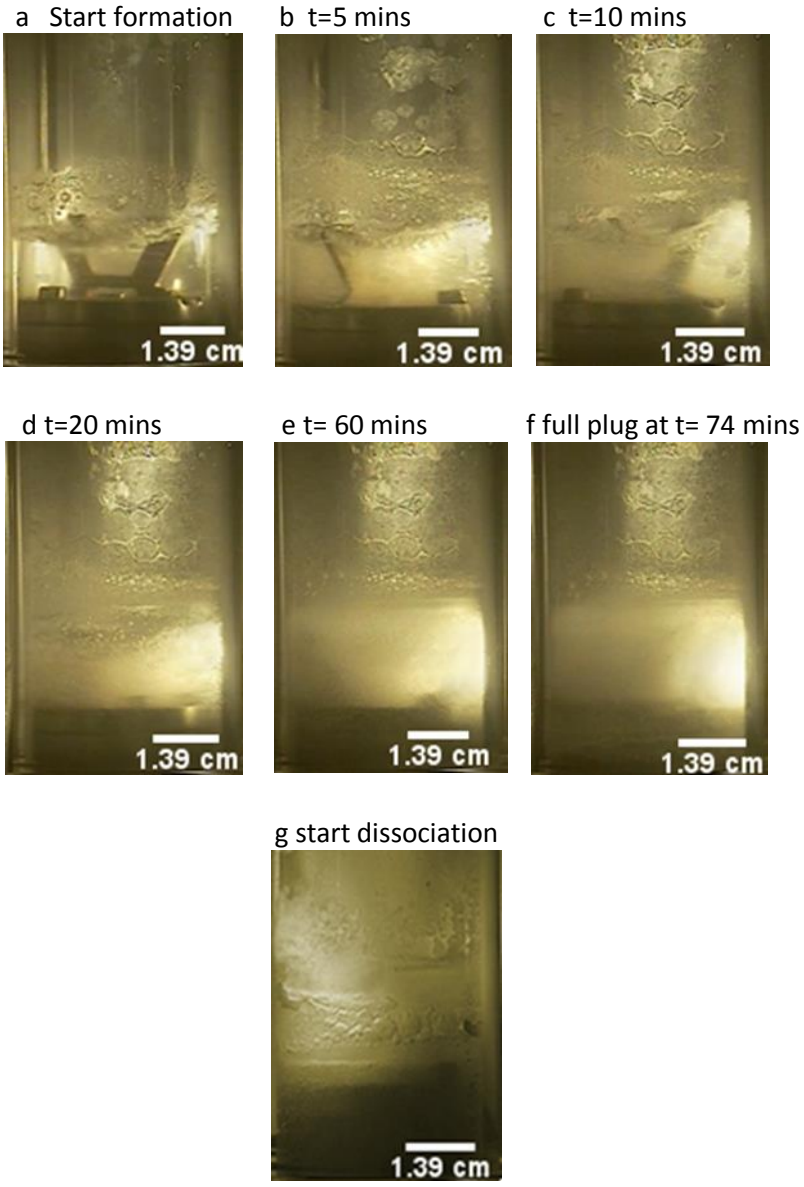


**Fig. 14.** Images captured during the experiments.

*3.3 Cage occupancies and model*

Fractional occupancies are calculated for methane and carbon dioxide mixtures in each cavity with the exception of carbon dioxide in the small cavity using equation (3) (Table 7). The guest/cavity size ratio for methane in the small cavity is 0.867 and 0.744 for the large. For carbon dioxide, the ratios are 1.018 and 0.874 for the small and large cavities respectively (Lederhos et al. 1993). Given that the carbon dioxide guest size

exceeds that of the small cavity, carbon dioxide adsorption is unlikely to occur. However, studies have shown that carbon dioxide occupation of the small cavity can occur with pure carbon dioxide gas (Ripmeester and Ratcliffe 1998; Circone et al. 2003). Methane has a far greater propensity towards the cavity due its optimal guest/cavity ratio and also far exceeds the carbon dioxide concentration in all gas mixtures. Methane was therefore assumed to dominate the occupation of small cavities, hence the occupation of carbon dioxide was negated.

An interesting observation is the greater overall occupation of large cavities. This is particularly noticeable at lower pressures. Methane and carbon dioxide are both capable of stabilising the large cavity as evidenced by their guest/cavity ratios, although carbon dioxide offers greater stability of the cavity. It makes sense that with two capable guest for the large cavity compared to one for the small cavity, $\theta_{i,l}$ will be greater than $\theta_{i,s}$. Methane has been shown to occupy the large cavity to a greater extent in the absence of carbon dioxide (Lee et al. 2013). It is likely that due to the relatively higher number of large cavities in sI hydrates (6 to 2 in a unit cell), methane will prefer the large cage. With more possible sites for methane guests to fill relative to small cages, a higher methane occupancy of large than small cages will result in greater free energy changes, and therefore greater lattice stabilisation.

Results also demonstrate an increase in $\theta_{i,j}$ for both sI cavities with pressure, which is in accordance with equation (3)., The filling of small cavities decreases with increased carbon dioxide concentration due to the accompanied reduction in methane partial pressure (and fugacity). Similarly, carbon dioxide filling of large cavities increases with $CO_2$ concentration and methane's small cavity occupation decreases to a minor extent. Likewise, the extent of large cavity occupation by carbon dioxide increases drastically and appears to be proportional to $CO_2$ concentration. This increase ultimately reduces methane's filling of large cavities. Greater inclusion of carbon dioxide in the lattice stabilises the hydrate structure because $CO_2$-water interactions are stronger than the $CH_4$-water interactions in the large cage (Sloan Jr and Koh 2008). Therefore the increase in $\theta_{CO2,l}$ promotes the hydrate equilibrium conditions.

The comparison of the experimental data measured in this work and the model calculations for various carbon dioxide + methane hydrates are illustrated in figure 15. It can be seen that the model results using the Kihara parameters are in good agreement with the experimental results at low to mid pressures. However, it should be noted that at higher pressures, the experimental equilibrium points are noticeably further to the right (higher temperature). This discrepancy could potentially be a consequence of the assumption that CO2 does not occupy small cages. Therefore results indicate that the model is accurate at lower pressures (<10 MPa), while it has considerable deviation at more extreme pressures where CO2 has a propensity (however small) to occupy the large cavities of structure I.

**Table 7**

Cage Occupancy Results.

| $CO_2$, mol% | P, MPa | $\theta_{C1,s}$ | $\theta_{C1,l}$ | $\theta_{CO2,l}$ | $\theta_{i,s}$ | $\theta i,l$ |
|---|---|---|---|---|---|---|
| 10 | 5.0 | 0.8468 | 0.8322 | 0.1288 | 0.8468 | 0.9611 |
| | 7.5 | 0.8924 | 0.8437 | 0.1300 | 0.8924 | 0.9737 |
| | 10 | 0.9172 | 0.8498 | 0.1303 | 0.9172 | 0.9802 |
| | 15 | 0.9434 | 0.8564 | 0.1303 | 0.9434 | 0.9867 |
| | 20 | 0.9573 | 0.8604 | 0.1297 | 0.9573 | 0.9901 |
| | 25 | 0.9659 | 0.8628 | 0.1293 | 0.9659 | 0.9921 |
| 16 | 5.0 | 0.8376 | 0.7605 | 0.2014 | 0.8376 | 0.9619 |
| | 7.5 | 0.8855 | 0.7712 | 0.2030 | 0.8855 | 0.9742 |
| | 10 | 0.9118 | 0.7771 | 0.2035 | 0.9118 | 0.9806 |
| | 15 | 0.9396 | 0.7831 | 0.2039 | 0.9396 | 0.9870 |
| | 20 | 0.9545 | 0.7874 | 0.2029 | 0.9545 | 0.9903 |
| | 25 | 0.9636 | 0.7908 | 0.2015 | 0.9636 | 0.9923 |
| 20 | 5.0 | 0.8306 | 0.7144 | 0.2479 | 0.8306 | 0.9623 |
| | 7.5 | 0.8806 | 0.7241 | 0.2505 | 0.8806 | 0.9746 |
| | 10 | 0.9077 | 0.7300 | 0.2508 | 0.9077 | 0.9808 |
| | 15 | 0.9368 | 0.7362 | 0.2509 | 0.9368 | 0.9872 |
| | 20 | 0.9523 | 0.7409 | 0.2495 | 0.9523 | 0.9904 |
| | 25 | 0.9619 | 0.7446 | 0.2478 | 0.9619 | 0.9924 |

Subscripts '*s*' and '*l*' refer to small and large cavities respectively.

Subscripts '*C1*' and '*CO2*' refer to methane and carbon dioxide respectively.

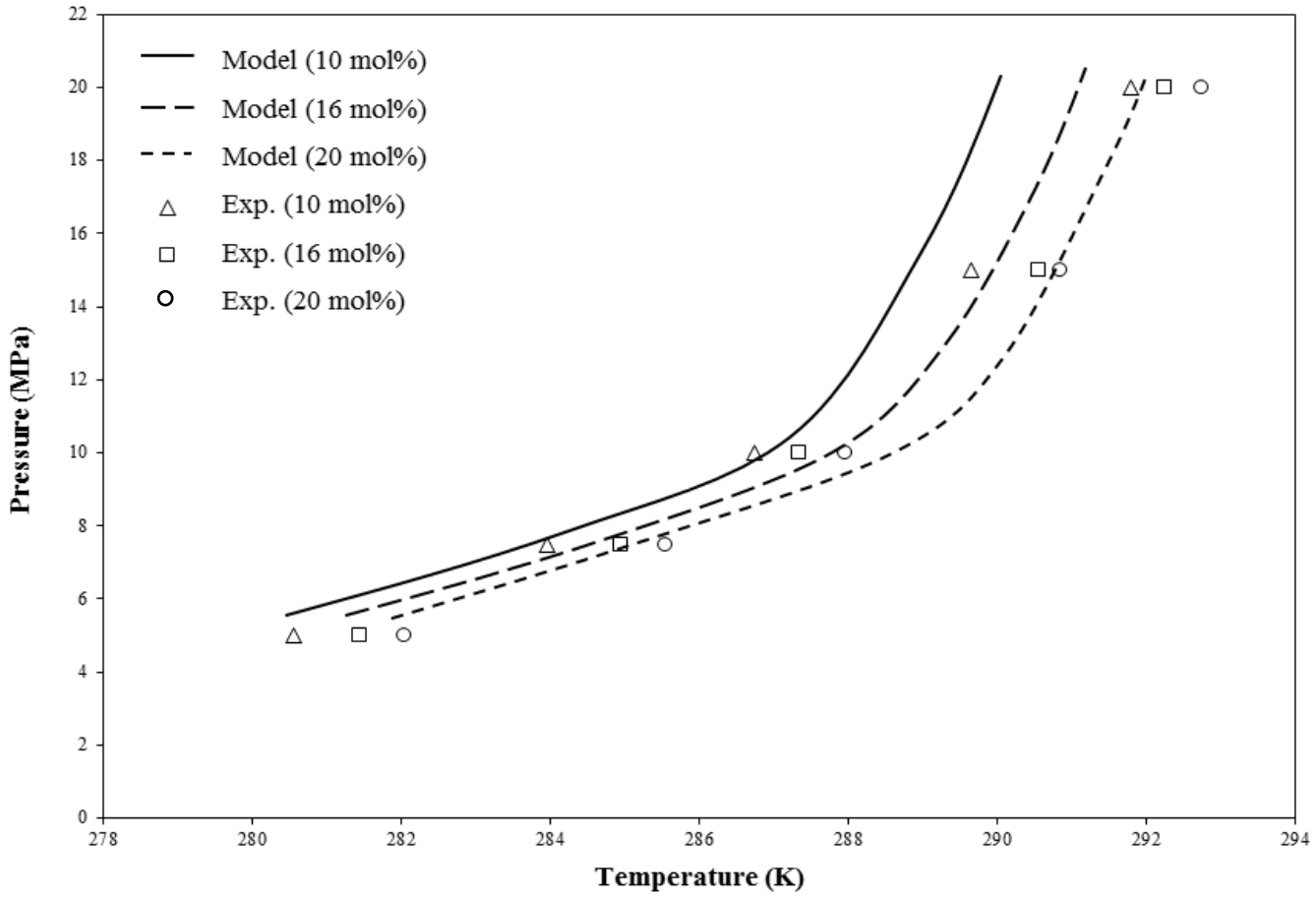


**Fig. 15.** Comparison of experimental methane – carbon dioxide hydrate dissociation points with model calculations. Numbers indicate $CO_2$ mole percentage in the mixture. Average relative deviations (ARDs) between the experimental data and the model results are 0.21%, 0.18% and 0.13% for the 10% $CO_2$ + 90% $CH_4$, 16% $CO_2$ + 84% $CH_4$ and 20% $CO_2$ + 80% $CH_4$ gas mixtures respectively.

## 4. Conclusions

The gas hydrate equilibrium conditions are of major significance in the energy sector due to the importance of gas hydrates as a potential alternative energy resource, as a means of $CO_2$ sequestration, also as a factor in global climate change and as a threat to flow assurance and gas production systems. Thus in this study, the hydrate equilibrium data for the systems carbon dioxide + methane + water, nitrogen + methane + water and carbon dioxide + nitrogen + water were experimentally measured in the PVT sapphire cell apparatus. Experiments were conducted at temperatures varying from 275.75K to 293.95K and pressures ranging from 5 MPa to 25 MPa. An acceptable agreement was found between the obtained experimental data

and literature data (Adisasmito, Frank, et al. 1991; Beltrán and Servio 2008; Dholabhai and Bishnoi 1994; Lu and Sultan 2008; Mohammadi et al. 2005; Sabil et al. 2014; Servio et al. 1999; Seo et al. 2001; Nakamura et al. 2003; Jhaveri and Robinson 1965). Specifically, we observed that at any given pressure the hydrate equilibrium temperature increased with increasing $CO_2$ mole percentage in the $CO_2$+$CH_4$ and $CO_2$+$N_2$ gas mixtures; while, increasing $N_2$ mole fraction in the $N_2$+$CH_4$ gas mixture reduced the hydrate equilibrium temperature at any given pressure. Furthermore, Motor current measurements were performed during gas hydrate formation and dissociation process; they showed that the motor current could be used as a gas hydrate formation and dissociation criterion, particularly in the cases where visual observations are not available. The occupancy calculations for the $CO_2$+$CH_4$ hydrate system showed that $CO_2$ stabilises the sI hydrate. Results also demonstrated that an increase in $CO_2$ gas composition resulted in a higher $CO_2$ hydrate composition. This helped confirm and explain the observed promotion of hydrate equilibrium conditions with increasing of $CO_2$ gas composition. A comparison between the experimental data and the model calculations for carbon dioxide + methane hydrates shows that the model can acceptably predict the hydrate equilibria at pressures lower than 10 MPa.

**Acknowledgement**

The authors would like to acknowledge the financial assistance provided by Curtin University through Clean Gas Technology Australia Research Centre (CGTA), Perth, W.A, Australia. Also, Dhifaf Sadeq acknowledges Iraqi Higher Education and Scientific Research Ministry, Iraq, for providing PhD scholarship at Curtin University.

**References**

Adeyemo, A., Kumar, R., Linga, P., Ripmeester, J., Englezos, P., 2010. Capture of carbon dioxide from flue or fuel gas mixtures by clathrate crystallization in a silica gel column. . Int. J. Greenhouse Gas Control 4, 478-485.

Adisasmito, S., Frank III, R. J., Sloan Jr, E. D., 1991. Hydrates of carbon dioxide and methane mixtures. J. Chem. Eng. Data 36, 68-71.

Adisasmito, S., Frank, R. J., Sloan, E. D., 1991. Hydrates of carbon dioxide and methane mixtures. J. Chem. Eng. Data 36, 68-71.

AlHarooni, K., Barifcani, A., Pack, D., Gubner, R., Ghodkay, V., 2015. Inhibition effects of thermally degraded MEG on hydrate formation for gas systems. J. Pet. Sci. Eng. 135,608-617.

Belandria, V., Eslamimanesh, A., Mohammadi, A. H., Théveneau, P., Legendre, H., Richon, D., 2011. Compositional analysis and hydrate dissociation conditions measurements for carbon dioxide+ methane+ water system. Ind. Eng. Chem. Res. 50, 5783-5794.

Belandria, V., Mohammadi, A. H., Richon, D., 2010. Phase equilibria of clathrate hydrates of methane+ carbon dioxide: New experimental data and predictions. Fluid Phase Equilib. 296, 60-65.

Beltrán, J. G., Servio, P., 2008. Equilibrium studies for the system methane+ carbon dioxide+ neohexane+ water. J. Chem. Eng. Data 53, 1745-1749.

Bishnoi, P. R., Natarajan, V., 1996. Formation and decomposition of gas hydrates. Fluid Phase Equilib. 117, 168-177.
Bruusgaard, H., Beltrán, J. G., Servio, P., 2008. Vapor− liquid water− hydrate equilibrium data for the system $N_2$+ $CO_2$+ $H_2O$. J. Chem. Eng. Data 53, 2594-2597.
Buffett, B. A., 2000. Clathrate hydrates. Annual Review of Earth and Planetary Sciences 28, 477-507.
Carroll, J., 2014. Natural gas hydrates: a guide for engineers. Gulf Professional Publishing.
Circone, S., Stern, L. A., Kirby, S. H., Durham, W. B., Chakoumakos, B. C., Rawn, C. J., Rondinone, A. J., Ishii, Y., 2003. $CO_2$ hydrate: synthesis, composition, structure, dissociation behavior, and a comparison to structure I $CH_4$ hydrate. The Journal of Physical Chemistry B 107, 5529-5539.
Dashti, H., Yew, L. Z., Lou, X., 2015. Recent advances in gas hydrate-based $CO_2$ capture. J. Nat. Gas Sci. Eng. 23, 195-207.
Delli, M. L., Grozic, J. L., 2014. Experimental determination of permeability of porous media in the presence of gas hydrates. J. Pet. Sci. Eng. 120, 1-9.
Dholabhai, P. D., Bishnoi, P. R., 1994. Hydrate equilibrium conditions in aqueous electrolyte solutions: mixtures of methane and carbon dioxide. J. Chem. Eng. Data 39, 191-194.
Englezos, P., 1993. Clathrate hydrates. Industrial & Engineering Chemistry Research 32, 1251-1274.
Erickson, D.D., 1983. Development of a Natural Gas Hydrate Prediction Computer Program. Master Thesis, Colorado School of Mines, Golden, CO.
Eslamimanesh, A., Mohammadi, A. H., Richon, D., Naidoo, P., Ramjugernath, D., 2012. Application of gas hydrate formation in separation processes: a review of experimental studies. The Journal of Chemical Thermodynamics 46, 62-71.
Fan, S.-S., Guo, T.-M., 1999a. Hydrate formation of $CO_2$-rich binary and quaternary gas mixtures in aqueous sodium chloride solutions. J. Chem. Eng. Data 44, 829-832.
Fan, S.-S., Guo, T.-M., 1999b. Hydrate formation of $CO_2$-rich binary and quaternary gas mixtures in aqueous sodium chloride solutions. J. Chem. Eng. Data 44, 829-832.
Goel, N., 2006. In situ methane hydrate dissociation with carbon dioxide sequestration: Current knowledge and issues. J. Pet. Sci. Eng. 51, 169-184.
Haghighi, H., Chapoy, A., Burgess, R., Tohidi, B., 2009. Experimental and thermodynamic modelling of systems containing water and ethylene glycol: Application to flow assurance and gas processing. Fluid Phase Equilib. 276, 24-30.
Herri, J.-M., Bouchemoua, A., Kwaterski, M., Fezoua, A., Ouabbas, Y., Cameirao, A., 2011. Gas hydrate equilibria for $CO_2$–$N_2$ and $CO_2$–$CH_4$ gas mixtures—Experimental studies and thermodynamic modelling. Fluid Phase Equilib. 301, 171-190.
Jhaveri, J., Robinson, D. B., 1965. Hydrates in the methane-nitrogen system. Can. J. Chem. Eng. 43, 75-78.
Kang, S.-P., Lee, H., Lee, C.-S., Sung, W.-M., 2001. Hydrate phase equilibria of the guest mixtures containing $CO_2$, $N_2$ and tetrahydrofuran. Fluid Phase Equilib. 185, 101-109.
Kim, D.-Y., Uhm, T.-W., Lee, H., Lee, Y.-J., Ryu, B.-J., Kim, J.-H., 2005. Compositional and structural identification of natural gas hydrates collected at Site 1249 on Ocean Drilling Program Leg 204. Korean J. Chem. Eng. 22, 569-572.
Kim, S. H., Do Seo, M., Kang, J. W., Lee, C. S., 2011. Hydrate-containing phase equilibria for mixed guests of carbon dioxide and nitrogen. Fluid Phase Equilib. 306, 229-233.
Kvamme, B., Graue, A., Buanes, T., Kuznetsova, T., Ersland, G., 2007. Storage of $CO_2$ in natural gas hydrate reservoirs and the effect of hydrate as an extra sealing in cold aquifers. INT. J. GREENHOUSE GAS CONTROL 1, 236-246.
Kvenvolden, K. A., 1988. Methane hydrate—a major reservoir of carbon in the shallow geosphere? Chem. Geol. 71, 41-51.
Lederhos, J., Christiansen, R., Sloan, E., 1993. A first order method of hydrate equilibrium estimation and its use with new structures. Fluid Phase Equilib. 83, 445-454.
Lee, J.-W., Kim, D.-Y., Lee, H., 2006. Phase behavior and structure transition of the mixed methane and nitrogen hydrates. Korean J. Chem. Eng. 23, 299-302.

Lee, S., Lee, Y., Park, S., Kim, Y., Cha, I., Seo, Y., 2013. Stability conditions and guest distribution of the methane+ ethane+ propane hydrates or semi clathrates in the presence of tetrahydrofuran or quaternary ammonium salts. The Journal of Chemical Thermodynamics 65, 113-119.

Linga, P., Kumar, R., Englezos, P., 2007. Gas hydrate formation from hydrogen/carbon dioxide and nitrogen/carbon dioxide gas mixtures. Chem. Eng. Sci. 62, 4268-4276.

Loh, M., Falser, S., Babu, P., Linga, P., Palmer, A., Tan, T. S., 2012. Dissociation of fresh-and seawater hydrates along the phase boundaries between 2.3 and 17 MPa. Energy Fuels 26, 6240-6246.

Lu, Z., Sultan, N., 2008. Empirical expressions for gas hydrate stability law, its volume fraction and mass-density at temperatures 273.15 K to 290.15 K. Geochem. J. 42, 163-175.

Makogon, Y., Holditch, S., Makogon, T., 2007. Natural gas-hydrates- A potential energy source for the 21st Century. J. Pet. Sci. Eng. 56, 14-31.

Makogon, Y. F., 2010. Natural gas hydrates–A promising source of energy. J. Nat. Gas Sci. Eng. 2, 49-59.

Mei, D.-H., Liao, J., Yang, J.-T., Guo, T.-M., 1996. Experimental and modeling studies on the hydrate formation of a methane+ nitrogen gas mixture in the presence of aqueous electrolyte solutions. Ind. Eng. Chem. Res. 35, 4342-4347.

Mohammadi, A. H., Anderson, R., Tohidi, B., 2005. Carbon monoxide clathrate hydrates: equilibrium data and thermodynamic modeling. AlChE J. 51, 2825-2833.

Moridis, G. J., 2008. Toward production from gas hydrates: current status, assessment of resources, and simulation-based evaluation of technology and potential. Lawrence Berkeley National Laboratory.

Najibi, H., Chapoy, A., Haghighi, H., Tohidi, B., 2009. Experimental determination and prediction of methane hydrate stability in alcohols and electrolyte solutions. Fluid Phase Equilib. 275, 127-131.

Nakamura, T., Makino, T., Sugahara, T., Ohgaki, K., 2003. Stability boundaries of gas hydrates helped by methane—structure-H hydrates of methylcyclohexane and cis-1, 2-dimethylcyclohexane. Chem. Eng. Sci. 58, 269-273.

Ohgaki, K., Makihara, Y., Takano, K., 1993. Formation of $CO_2$ Hydrate in Pure and Sea Waters. J. Chem. Eng. Jpn. 26, 558-564.

Park, K.-n., Hong, S. Y., Lee, J. W., Kang, K. C., Lee, Y. C., Ha, M.-G., Lee, J. D., 2011. A new apparatus for seawater desalination by gas hydrate process and removal characteristics of dissolved minerals ($Na^+$, $Mg_2^+$, $Ca_2^+$, $K^+$, $B_3^+$). Desalination 274, 91-96.

Ripmeester, J. A., Ratcliffe, C. I., 1998. The diverse nature of dodecahedral cages in clathrate hydrates as revealed by 129Xe and 13C NMR spectroscopy: $CO_2$ as a small-cage guest. Energy & fuels 12, 197-200.

Sabil, K. M., Nasir, Q., Partoon, B., Seman, A. A., 2014. Measurement of H–LW–V and Dissociation Enthalpy of Carbon Dioxide Rich Synthetic Natural Gas Mixtures. J. Chem. Eng. Data 59, 3502-3509.

Seo, Y.-T., Kang, S.-P., Lee, H., Lee, C.-S., Sung, W.-M., 2000. Hydrate phase equilibria for gas mixtures containing carbon dioxide: a proof-of-concept to carbon dioxide recovery from multicomponent gas stream. Korean J. Chem. Eng. 17, 659-667.

Seo, Y.-T., Lee, H., Yoon, J.-H., 2001. Hydrate phase equilibria of the carbon dioxide, methane, and water system. J. Chem. Eng. Data 46, 381-384.

Servio, P., Lagers, F., Peters, C., Englezos, P., 1999. Gas hydrate phase equilibrium in the system methane–carbon dioxide–neohexane and water. Fluid Phase Equilib. 158, 795-800.

Sfaxi, I. B. A., Belandria, V., Mohammadi, A. H., Lugo, R., Richon, D., 2012. Phase equilibria of $CO_2$+ $N_2$ and $CO_2$+ $CH_4$ clathrate hydrates: Experimental measurements and thermodynamic modelling. Chem. Eng. Sci. 84, 602-611.

Sloan, E. D., 2003. Clathrate hydrate measurements: microscopic, mesoscopic, and macroscopic. The Journal of Chemical Thermodynamics 35, 41-53.

Sloan, E. D., Koh, C. A., Sum, A., 2010. Natural gas hydrates in flow assurance. Gulf Professional Publishing.

Sloan Jr, E. D., Koh, C., 2008. Clathrate hydrates of natural gases. CRC press.

Smith, C., Barifcani, A., Pack, D., 2015. Gas hydrate formation and dissociation numerical modelling with nitrogen and carbon dioxide. J. Nat. Gas Sci. Eng. 27, 1118-1128.
Smith, C., Barifcani, A., Pack, D., 2016. Helium substitution of natural gas hydrocarbons in the analysis of their hydrate. J. Nat. Gas Sci. Eng. 35, 1293-1300.
Sun, S.-C., Liu, C.-L., Meng, Q.-G., 2015. Hydrate phase equilibrium of binary guest-mixtures containing CO 2 and N 2 in various systems. The Journal of Chemical Thermodynamics 84, 1-6.
Sun, Z.-g., Wang, R., Ma, R., Guo, K., Fan, S., 2003. Natural gas storage in hydrates with the presence of promoters. Energy Convers. Manage. 44, 2733-2742.
Taheri, Z., Shabani, M. R., Nazari, K., Mehdizaheh, A., 2014. Natural gas transportation and storage by hydrate technology: Iran case study. J. Nat. Gas Sci. Eng. 21, 846-849.
Tohidi, B., Anderson, R., Clennell, M. B., Burgass, R. W., Biderkab, A. B., 2001. Visual observation of gas-hydrate formation and dissociation in synthetic porous media by means of glass micromodels. Geology 29, 867-870.
Tohidi, B., Burgass, R., Danesh, A., Østergaard, K., Todd, A., 2000. Improving the accuracy of gas hydrate dissociation point measurements. Ann. N.Y. Acad. Sci. 912, 924-931.
Ueno, H., Akiba, H., Akatsu, S., Ohmura, R., 2015. Crystal growth of clathrate hydrates formed with methane+ carbon dioxide mixed gas at the gas/liquid interface and in liquid water. New J. Chem. 39, 8254-8262.
Unruh, C. H., Katz, D. L., 1949. Gas hydrates of carbon dioxide-methane mixtures. Journal of Petroleum Technology 1, 83-86.
Van Cleeff, A., Diepen, G., 1960. Gas hydrates of nitrogen and oxygen. Recl. Trav. Chim. Pays-Bas 79, 582-586.
Van der Waals, J. H., Platteeuw, J. C., 1959. Clathrate solutions. Adv. Chem. Phys. 2, 1−57
Wood, D. A., 2015. Gas hydrate research advances steadily on multiple fronts: A collection of published research (2009–2015). J. Nat. Gas Sci. Eng., A1-A8.
Xie, Y., Li, G., Liu, D., Liu, N., Qi, Y., Liang, D., Guo, K., Fan, S., 2010. Experimental study on a small scale of gas hydrate cold storage apparatus. Applied Energy 87, 3340-3346.